A&A 391, 317–329 (2002)
DOI: 10.1051/0004-6361:20020745

Astronomy & Astrophysics

The role of magnetic bald patches in surges and arch filament systems

C. H. Mandrini[1], P. Démoulin[2], B. Schmieder[2,3], Y. Y. Deng[4], and P. Rudawy[5]

[1] Instituto de Astronomía y Física del Espacio, IAFE, CC.67, Suc.28, 1428 Buenos Aires, Argentina*
[2] Observatoire de Paris, LESIA, FRE 2461 (CNRS), 92195 Meudon Cedex, France
e-mail: pascal.demoulin@obspm.fr
[3] Institute of Astrophysics, 0315 Blindern, Oslo 3, Norway
[4] Beijing Astronomical Observatory, Beijing 100080, PR China
[5] Astronomical Institute, Wroclaw University, 51-622 Wroclaw, Poland

Received 1 February 2002 / Accepted 16 April 2002

Abstract. The short-lived active region (AR) NOAA 7968 was thoroughly observed all along its disk transit (June 3 to 10, 1996) from space and from the ground. During the early stage of its evolution, flux emerged in between the two main polarities and arch filament systems (AFS) were observed to be linked to this emergence. New bipoles and a related surge were observed on June 9. We have modeled the magnetic configuration of AR 7968 using a magnetohydrostatic approach and we have analyzed its topology on June 6 and June 9 in detail. We have found that some of the AFS and the surge were associated with field lines having dips tangent to the photosphere (the so called "bald patches", BPs). Two interacting BP separatrices, defining a separator, have been identified in the configuration where these very different events occurred. The observed evolution of the AFS and the surge is consistent with the expected results of magnetic reconnection occuring in this magnetic topology, which is specific to 3D configurations. Previously BPs have been found to be related to filament feet, small flares and transition region brightenings. Our results are evidence of the importance of BPs in a much wider range of phenomena, and show that current layers can be formed and efficiently dissipated in the chromosphere.

Key words. magnetohydrodynamics (MHD) – methods: miscellaneous – Sun: activity – Sun: chromosphere – Sun: magnetic fields

1. Introduction

Under typical coronal conditions the magnetic field is force-free and frozen into the plasma almost everywhere in solar active regions. Separatrix surfaces or separatrices are an exception where current layers may be formed. Apart from the case in which magnetic nulls are present in the corona, separatrices can only appear in a magnetic volume when some field lines are tangentially touching the boundary (i.e. the photosphere). This can happen along portions of the inversion line for the component of the magnetic field normal to this boundary. These portions are the so-called "bald patches" or BPs (Titov et al. 1993). Above a BP the field lines are curved up, and the horizontal component of the magnetic field (the one on the photospheric plane) crosses the inversion line from the negative to the positive polarity, i.e. in the opposite way as compared to the normal portions of this line. The criterion for the existence of BPs was first given by Seehafer (1986), and in more detail by Titov et al. (1993).

BPs are interesting topological features for several reasons. They define separatrices where current layers can develop (see e.g. Low & Wolfson 1988; Vekstein et al. 1991; Aly & Amari 1997). The separatrices starting at two distinct BPs may intersect defining a topologically special field line, called separator, where magnetic reconnection is quite plausible (Bungey et al. 1996). In this aspect BPs are important since, contrary to the traditional definition, such separator does not connect two null points. Besides, during the evolution of some magnetic configurations, BPs may be precursors of the emergence of a null point in the coronal field (Bungey et al. 1996), being again associated with reconnection processes. Furthermore, BPs are thought to be the locations where chromospheric material can be lifted up and, so, they can be also linked to processes occurring in prominences (Titov et al. 1993; Aulanier & Démoulin 1998). Recently, Titov & Démoulin (1999) extended previous studies on BPs to a non-linear force-free magnetic configuration representing a twisted flux tube.

There is some evidence of the presence of BPs in flares, the first examples were given implicitly by

Send offprint requests to: C. H. Mandrini,
e-mail: mandrini@iafe.uba.ar
* Member of the Carrera del Investigador Científico, CONICET, Argentina.

Seehafer & Staude (1980) and Seehafer (1985). Aulanier et al. (1998a) found a close correspondence between the BP separatrices and the Hα and X-ray emissions in a small flare; Delannée & Aulanier (1999) studied a flare associated with BPs, which could have been the origin of a coronal mass ejection. More recently, Fletcher et al. (2001) found that transition region brightenings associated with BPs had abundances close to photospheric values.

AR NOAA 7968 was the target of a special coordinated observing campaign (Joint Observing Program, JOP 17) involving the instruments aboard the Solar and Heliospheric Observatory (SoHO), *Yohkoh*, and ground-based observatories. This AR was relatively short-lived and, thus, it was observed from its birth to its decay phase (Deng et al. 1999). In this work we analyze two different kinds of events that imply the intrusion of chromospheric plasma into the corona: the formation of Arch Filament System (AFS) and surges.

Emergence of flux is frequently observed in the solar atmosphere. This emergence, when large enough, can give rise to the formation of active regions (ARs). In the early phase of its evolution, an AR is characterized at chromospheric level by the presence of very low and dark filaments, the AFS. These systems can be observed over several days, while the individual arches last only a few tens of minutes. As the flux emerges, new arches are formed while the older ones expand in the atmosphere (Alissandrakis et al. 1990). On the other hand, hot loops are observed overlaying the AFS at coronal heights (Malherbe et al. 1998 and references therein). We describe here the evolution of some individual arches observed in Hα during the growth of AR 7968 (June 6, 1996) and, comparing them to extrapolated magnetic field lines, we discuss their evolution in terms of the topological changes in the magnetic field.

The physical mechanisms, that are involved in chromospheric mass ejections called surges, are not clearly understood. The surge may be driven by a high pressure gradient in a magnetic tube, as first proposed by Steinolfson et al. (1979) or it may be due to magnetic energy release through reconnection (Heyvaerts et al. 1977; Shibata et al. 1992). Rust (1968) found an observational relationship between AFS and surges. Kurokawa & Kawai (1993) showed that Hα surges are seen in the early stages of flux emergence, and concluded that they are produced by magnetic reconnection between the emerging flux region and the pre-existing surrounding field (see also Schmieder et al. 1996). Canfield et al. (1996) followed the same ideas to propose a phenomenological model to explain surges and X-ray jets in an AR. We discuss here the origin of a surge which was observed on June 9, 1996, in AR 7968. The topological analysis of the magnetic configuration suggests that the surge is driven by magnetic reconnection, but unlike the examples just mentioned energy release seems to be linked to the presence of a separator created by the interaction of two BPs.

In Sect. 2, we list the observations included in the present analysis and we describe briefly the approach used to model the observed magnetic field. After this, we present the chromospheric events: the AFS, in Sect. 3, and the surge, in Sect. 4. We describe their characteristics in Sects. 3.1 and 4.1, and we explain their evolution in terms of the topology of the magnetic field in Sects. 3.3, 3.4, and 4.2, respectively. Finally, we discuss our results and conclude (Sect. 5). Preliminary results of this work have been published in Mandrini et al. (1999a, 1999b).

2. The observations and the magnetic field model

2.1. The data

NOAA AR 7968 appeared on June 3, 1996, and was observed to decay ~5 days later, on June 9. The full set of multi-wavelength observations obtained during the AR disk passage have been described in detail by Deng et al. (1999). For the present study we have used data from the Michelson Doppler Imager (SoHO/MDI), together with Hα filtergrams and velocity maps.

The SoHO/MDI observations of this region consist of full disk longitudinal magnetograms taken with a time cadence of 96 min. The spatial resolution is 1.96″ (Scherrer et al. 1995). The noise threshold is 10 G, which is reduced to 5 G integrating several magnetograms along 5 min. Because of problems in the telemetry, some of the images have stripes with no data. We have used only those which had a small number of missing pixels to extrapolate the magnetic field. These data were replaced by interpolating between neighboring values.

Hα filtergrams were taken with the Large Coronagraph at Bialków Observatory (Poland) with a cadence of less than one hour. The available data cover around ten hours per day on June 6 and June 7. The FWHM of the filter is 0.5 Å and the field of view is $\sim 5.83' \times 3.67'$. The pixel size is 0.433″ and the spatial resolution is less than ~1″.

Hα observations were also obtained at Bialków using the Multi-Channel Subtractive Double Pass (MSDP) spectrograph (Mein 1991) on June 9. This instrument provides simultaneously 2D data at nine spectral positions covering the Hα line profile, with a field of view of up to $41'' \times 325''$. The Hα profiles were reconstructed for each pixel of the region using spline functions. The quiet regions are used to define a mean profile, which is taken as the reference profile; its line centre wavelength, λ_0, defines with a good approximation the line centre for the static plasma. The Dopplershift is computed considering the displacement of the bisector of the line profile with respect to the λ_0 reference wavelength (chord method). Intensity maps, $I(\lambda)$, were computed using the MSDP data to simulate filter-like data at fixed wavelengths ($\lambda_0 \pm \Delta\lambda$). The difference of these intensity maps in blue and red wings ($I(\lambda_0 - \Delta\lambda) - I(\lambda_0 + \Delta\lambda)$) provides qualitative information on the plasma motions along the line of sight. For qualitative analysis, we have used the just mentioned difference because the contrast is better than the one in Dopplershift maps. For quantitative results we have used the Dopplershifts obtained with the chord method.

2.2. Brief description of the photospheric evolution

AR 7968 appeared on the disk on June 3 as a negative polarity spot in a bipolar facular region. By June 5, the area of the spot was increasing and several small positive spots appeared and were seen to follow it. These positive spots gathered forming a mainly bipolar AR with an inversion line heading in the North-South direction. Along June 6, positive and negative

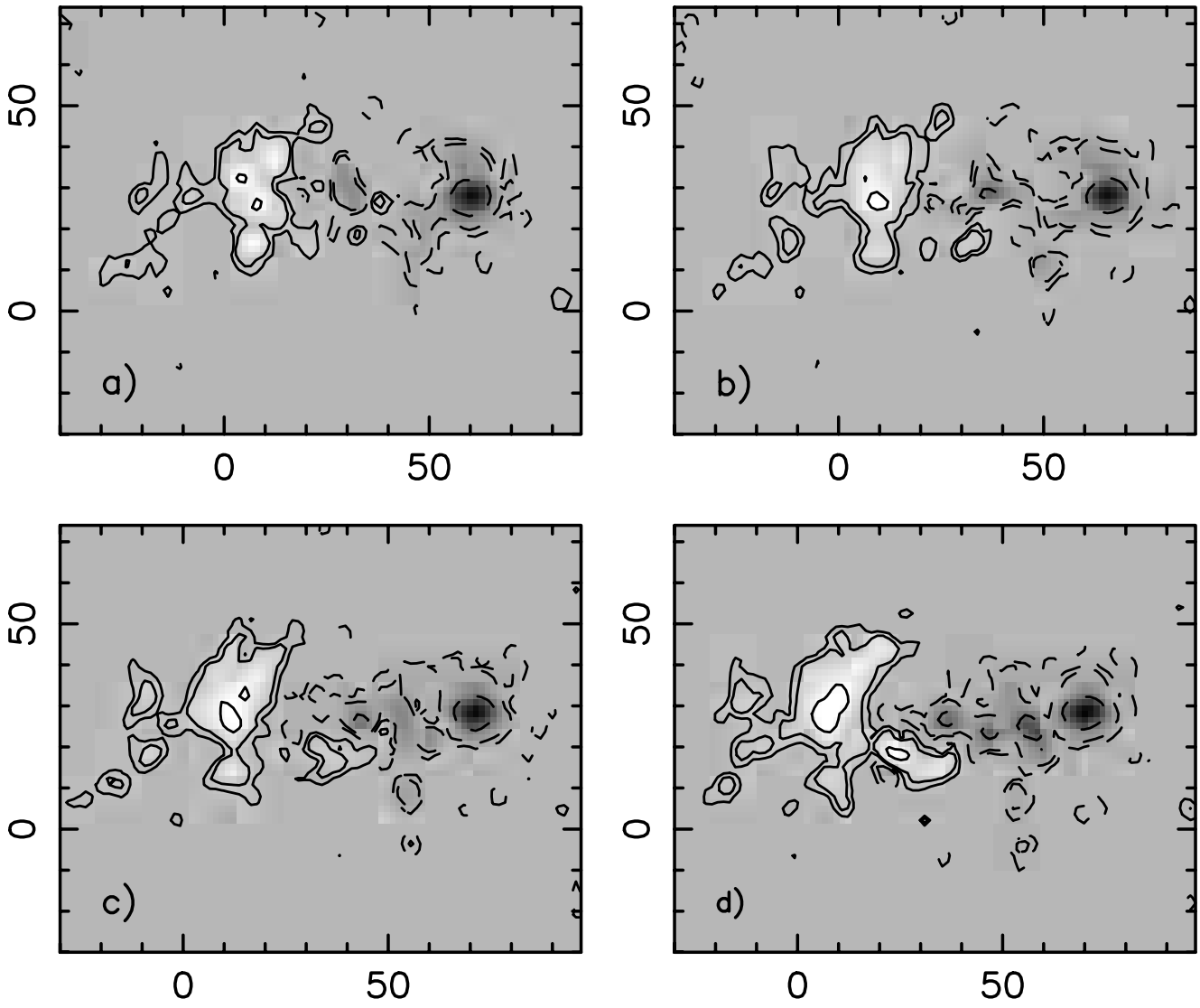

Fig. 1. The photospheric line of sight component of the magnetic field in AR 7968 during June 6. Sections of MDI full disk observations taken at: **a)** 06:28 UT, **b)** 11:16 UT, **c)** 16:04 UT and **d)** 22:28 UT. North is up and West is to the right in this and following figures (unless indicated differently). The data represented in grey scale are saturated above/below 500 G/−1300 G, the isocontours correspond to ±40, 100 and 500 G (positive/negative values are shown with continuous/dashed lines). The horizontal and vertical axis (x, y) are in Mm.

fluxes emerged continuously in between the strongest polarities (Fig. 1) in such a way that, by the end of the day, part of the AR inversion line was oriented in the East-West direction. At the same time some small opposite polarities were observed cancelling.

After the continuous and fast flux emergence on June 6, the total positive and negative fluxes grew at a slower rate during June 7 and June 8. By June 9, the AR magnetic flux started to decrease. Figure 2a shows the line of sight magnetic field as observed on June 8, while Figs. 2b–d depict the evolution of the field during June 9. A new negative flux concentration appeared at the South of the main positive polarity, this region was accompanied by a positive zone having a lower magnetic field intensity (located at ≈25 Mm to the South of the negative polarity). AR 7968 reached the West limb on June 11 and died while being unseen. This region was characterized by a very low level of activity along its life time, only small X-ray (class B) flares and surge ejections occurred during its transit across the solar disk.

2.3. Modelling the magnetic field

To investigate the relation between the evolution of the magnetic field and the morphological changes at chromospheric level, we have modeled the field of AR 7968. We have extrapolated the observed line of sight component of the photospheric field to the corona using a linear magnetohydrostatic (LMHS) approximation, which is appropriate in our case because the plasma velocity is in general much smaller than the Alfvén speed. A complete description of the equations governing the MHS equilibrium (Low 1991, 1992), and of the numerical approach followed to solve them can be found in Aulanier et al. (1998a) and Fletcher et al. (2001). In a cartesian (x, y, z) system of coordinates, where the z axis is chosen to be normal to

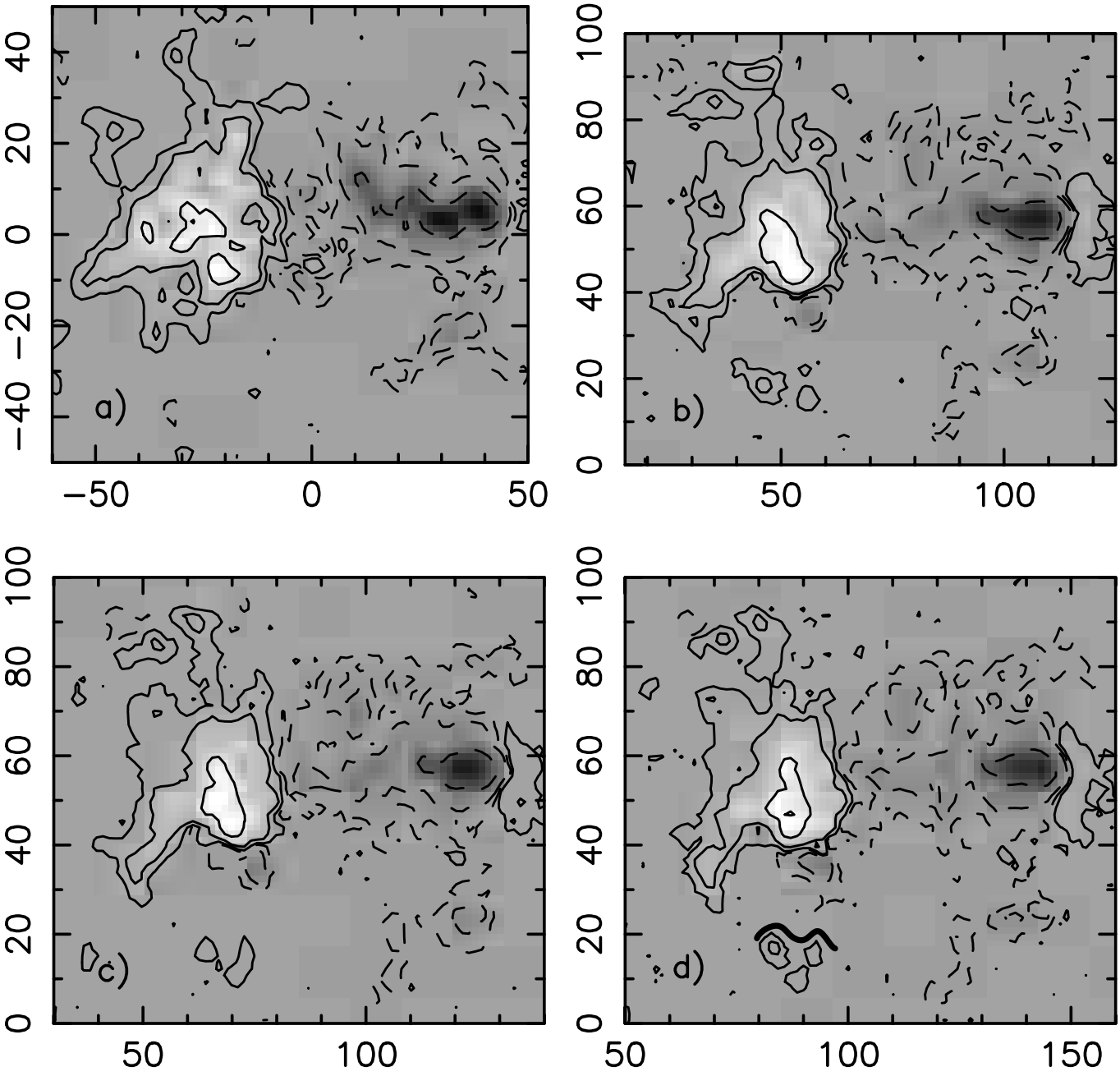

Fig. 2. The line of sight component of the magnetic field during June 8 and June 9. AR 7968 as observed with MDI at: **a)** 01:40 UT on June 8, and **b)** 01:40 UT, **c)** 04:52 UT and **d)** 08:40 UT on June 9. The data in grey scale are saturated above/below 700 G/−1200 G, the isocontours correspond to ±20, 100 and 500 G with the same convention as in Fig. 1. The thick black line in **d)** shows the inversion line between the negative (above) and positive (below) polarities of the new bipole (see Sect. 2.2).

the photosphere and $z = 0$ at the photospheric level, we arrive to the following equation:

$$\boldsymbol{\nabla} \times \boldsymbol{B} = \alpha \boldsymbol{B} + f(z) \boldsymbol{\nabla} B_z \times \boldsymbol{u}_z \tag{1}$$

where α is supposed to be a constant, as in the linear force-free approximation, and $f(z) = a \exp(-z/H)$. The interaction between the magnetic field and the plasma is taken into account through $f(z)$. The parameter a is the ratio between the plasma pressure depletion and the magnetic pressure, $B_z^2/2\mu_0$ (see references above). The vertical extension of the influence of the plasma is given by the scale-height H. Low (1992) showed that in some cases H can be equal or close to an isothermal pressure scale-height. Here, we take $H = 2$ Mm as a typical scale-height for the chromosphere, and we choose $a = 1$, which is its largest possible value (see the discussion in Aulanier et al. 1998a).

Given a and H, the model depends only on the free parameter α. We have selected the value of α in such a way that the computed coronal field lines match the shape of the loops observed with the Extreme Ultraviolet Imaging Telescope (SoHO/EIT) in 195 Å (see Deng et al. 1999). We have used SoHO/EIT images at times close to the MDI magnetograms to determine the value of α. The best fit on June 6 and 7 was

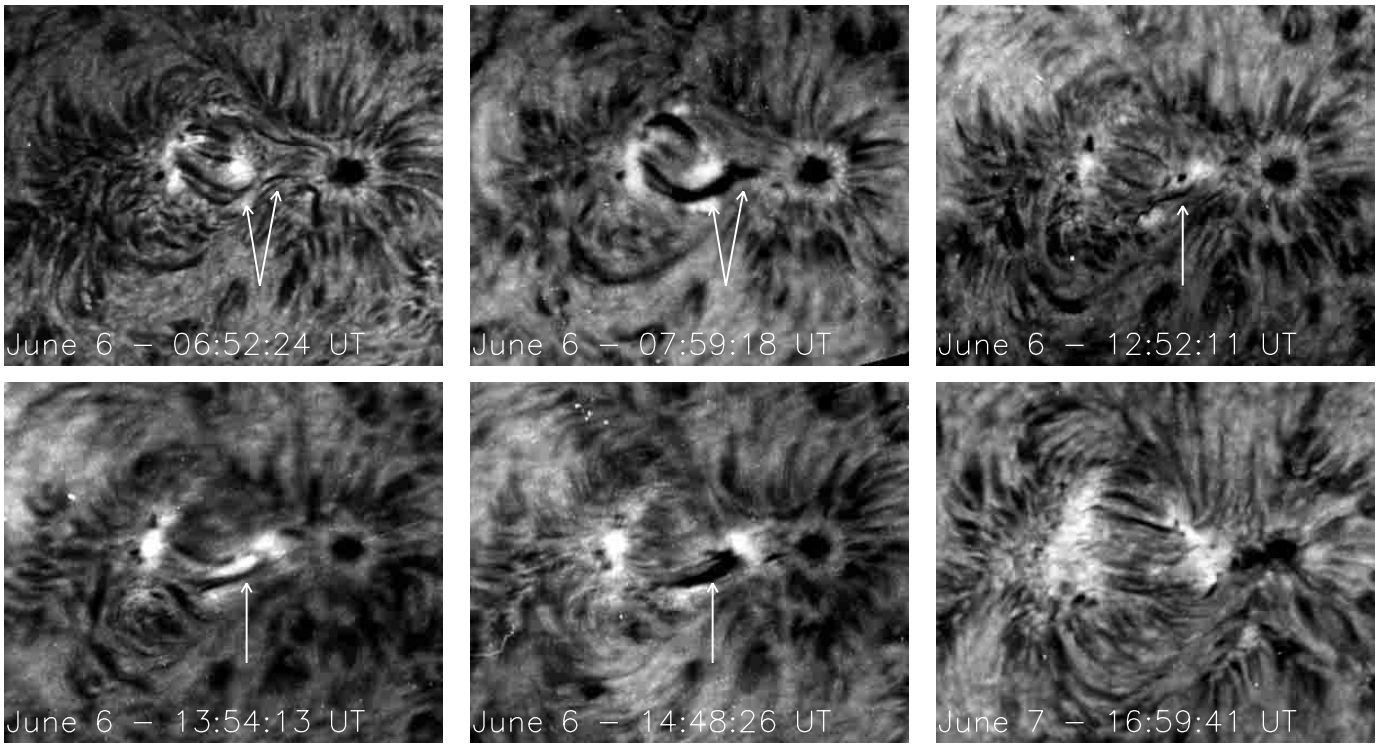

Fig. 3. Evolution of AR 7968 as observed in Hα on June 6–7, 1996 (filtergrams in Hα line center, see Sect. 2.1). Notice the changes, marked with arrows (see text), observed in the central dark arches from 06:52:24 UT to 07:59:18 UT and from 12:52:11 UT to 14:48:26 UT. The field of view is the same as in Fig. 1.

found for $\alpha = -0.0063\,\mathrm{Mm}^{-1}$, indicating that the configuration is close to potential. For June 9 the global magnetic configuration of AR 7968 is best represented by $\alpha = 0$.

3. The dark arches in the early phase of AR 7968

3.1. Evolution of the arches

The evolution of the photospheric field (Fig. 1) is followed at the chromospheric level by visible changes in heavily absorbing arches or AFS. Figure 3 shows the evolution in Hα as observed at Bialków Observatory. We have identified several examples along June 6 during which single short fibrils evolve into longer and darker ones. In other cases, two AFSs or fibrils evolve into a single group of chromospheric dark arches. We select two examples of the just described behavior in Fig. 3. In the first one, two short arches join either the positive or the negative portion of the new emerging flux to the preceding and following main spots. These two arches evolve in a longer and darker one. This can be seen when comparing the image at 06:52:24 UT with the one at 07:59:18 UT (arrows in Fig. 3 at those times). In the second example, a short arch joining new positive and negative flux elongates in the same direction and becomes darker, compare the image at 12:52:11 UT with those at 13:54:13 UT and 14:48:26 UT (arrow in Fig. 3 at those times).

Clearly many topological rearrangements have taken place in the chromosphere during this dynamic period. By June 7, flux emergence in between the two main spots has significantly decreased and the Hα image presents the familiar picture of long magnetic flux tubes anchored in opposite polarity regions (Alissandrakis et al. 1990; Georgakilas et al. 1990; Mein et al. 1996 and references therein), roughly parallel to the major axis of the region (see the last image in Fig. 3). All along this period the AR was overlaid by hot coronal loops seen in images taken with SoHO/EIT and the Soft X-ray Telescope (*Yohkoh*/SXT) (see Deng et al. 1999). Unluckily, MSDP images are not available for this early phase; therefore, we cannot follow plasma motions in the dark arches.

3.2. Classical model

The emergence of flux at the photosphere has often been associated with the observations of AFS at the chromospheric level (e.g. Chou & Zirin 1988; Alissandrakis et al. 1990; Tsiropoula et al. 1992 and references therein). These observations show Hα blue-shifts at the top of the AFS, while red-shifts are seen along their legs; this indicates that the cold plasma moves up in the central part and flows down at the footpoints. AFS are then interpreted as classical Ω loops which ascend into the atmosphere as the new flux emerges (see e.g. Georgakilas et al. 1990; Mein et al. 1996). During the emergence, the cold material inside the magnetic loops looses gravitational equilibrium and flows away along both legs, as in the so-called "leaky bucket" model (Schmieder et al. 1991).

The aim of this work is not to challenge the above well established facts, but rather to analyze examples that are more complex than this standard view. Indeed, part of the observed AFSs in AR 7968 fit well in this classical view.

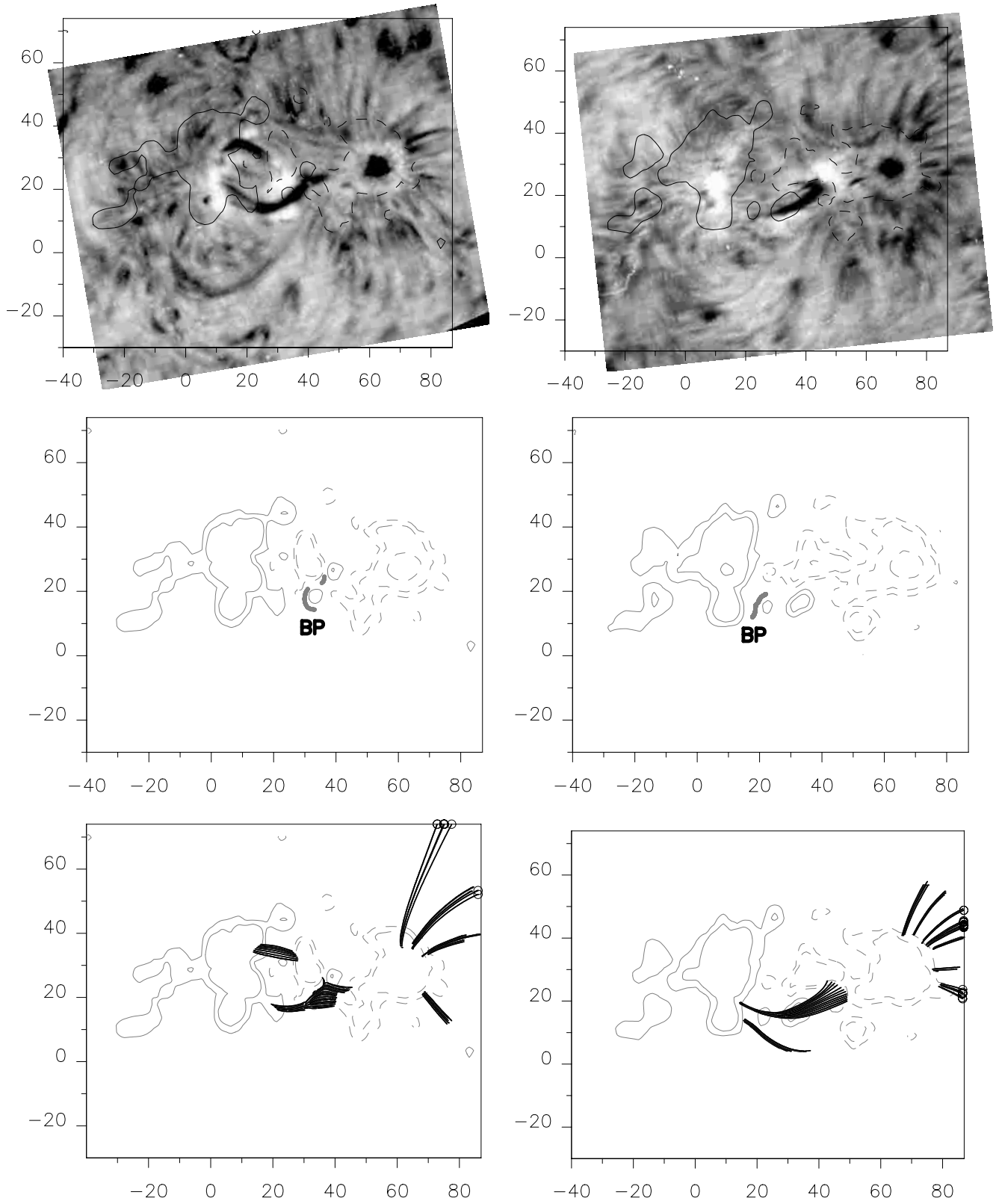

Fig. 4. Observations and models of AR 7968 on June 6. Panels on the left correspond to the MDI magnetogram taken at 06:28 UT, while the ones on the right to the magnetogram taken at 11:16 UT. Top panels show the Hα images at 07:59:18 UT and at 14:48:26 UT (see Fig. 3) and the ±40 G isocontours of MDI. The locations of the BPs associated with some of the observed AFS are shown in the central panels; while in the bottom panels we have drawn field lines, issued from the BPs, whose shapes follow the shapes of the AFS. Field lines representing fibrils not related to BPs have also been plotted. The conventions for the field and axis are the same as in Fig. 1.

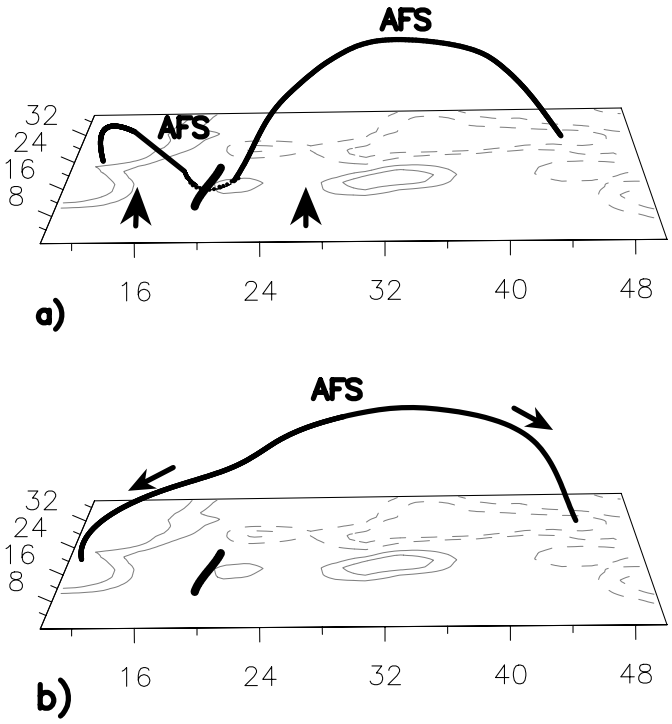

Fig. 5. A sketch of the evolution of the dark chromospheric arches associated with BPs. The magnetogram shown is the one taken at 11:16 UT on June 6 and the BP, which is shown as a dark thick line on the photospheric plane, is the one found at that time (see Fig. 4, right column). **a)** Chromospheric plasma accumulates in the curved upward portion of the field lines at BPs. Emergence of the AFS (as shown by the large arrows) at both sides of the BP favors the lift up of the plasma. **b)** As the dip becomes flatter, plasma can flow along the field lines (as shown by the small arrows) forming the elongated dark arches. Magnetic reconnection is also expected to occur along the separatrix associated with the BP because of photospheric motions, this favors the transition from the configuration in **a)** to the one in **b)** (see Sect. 3.3).

One example is shown in the left column of Fig. 4: the top AFS (very dark on the top-left panel) is approximately reproduced by the computed field lines (shown on the bottom-left panel). These field lines are arch-like, i.e. as in the standard view. However, we cannot confirm the classical blue/red shifted pattern of AFS since, as mentioned above, no MSDP observations are available at the time of flux emergence for AR 7968.

The magnetic field model allows us also to fit the Hα fibrils around the sunspot (see several examples in Fig. 4). All these fibrils have a typical arch-like (or loop-like) shape, as classically proposed based on observations and incorporated in fibril models; however, the flow pattern is different from that in AFS, it is a siphon flow (see e.g. Thomas 1988; Surlantzis et al. 1994, and references therein).

The examples presented above show that our model of the magnetic field is able to reproduce the standard magnetic configurations for the observed arch-like Hα features. However, some of the Hα features are not arch-like and, thus, they have non-classical magnetic configurations. It is important to notice that this is unlikely to be a special characteristic of our magnetic extrapolation. In particular, the BPs found (and shown in Figs. 4, 6 and 8) are also present in a potential magnetic field model of the AR (i.e. without electric currents, $\alpha = 0$, and without plasma forces, $a = 0$). As the effect of the presence of the plasma (represented by the value of a) is increased, the spatial extension of the BPs and of their associated separatrices slightly increases. For $a \approx 1$ we just find a better agreement between the computed field lines and the observations, as it was obtained before in very different contexts, e.g. for filament fine structures (Aulanier et al. 1998b), a small low lying flare (Aulanier et al. 1998a), and UV brightenings (Fletcher et al. 2001). In what follows, we present only the non-standard magnetic configurations found.

3.3. AFS with one BP

BPs are places where relatively cold material can be supported (Titov et al. 1993; Aulanier & Démoulin 1998), so their locations, and related portion of the field lines, are likely to be observed as dark regions in Hα. We have computed the location of BPs for the magnetic field model on June 6. Figures 4 (central panels) show the locations of BPs for the magnetic field at 06:28 UT and 11:16 UT. Several field lines issued from these BPs have been drawn in the bottom figures. It can be seen that the shapes of these lines are in good agreement with some of the dark arches observed in the top Hα images. The peculiar shape of the AFS shown in the left column is partially reproduced; the magnetic model fails to represent its full extension towards the left, probably because of the presence of local electric currents, which are not taken into account in the extrapolation.

The simplest mechanism through which the short arches (observed at 06:52:24 UT and at 12:52:11 UT) could evolve in darker elongated structures is the upward motion of the magnetic loops, as illustrated in Fig. 5. Dense material can be accumulated in the dipped portions of the field lines. As they move up in the atmosphere, because of the continuous flux emergence observed during this period, the dips would become more shallow and the plasma could flow along the field lines resulting in the formation of longer arches. This mechanism is similar to the one proposed by Spruit et al. (1987) for the emergence of U-loops at the photospheric level, but taking place in the lower chromosphere (see also Low & Hundhausen 1995; Rust & Kumar 1994). Deng et al. (2000) have recently interpreted the formation of long dark AFS in Hα in a similar way, though no magnetic field topology analysis has been done in this case. The main problem with this mechanism is that it supposes that the magnetic force is strong enough to overcome the gravity force, which is not obvious below the middle chromosphere (see e.g. Spruit et al. 1987; Titov et al. 1993).

The above problem of mass loading in ideal MHD can be solved by the following mechanism. As the arches evolve because of photospheric changes, magnetic reconnection is expected to occur along the separatrices associated with the BP. Several authors have discussed the possibilities for the formation of current sheets in BP configurations during a quasi-static evolution driven by photospheric motions (see Titov & Démoulin 1999, for a discussion). For example,

in configurations invariant by translation shearing motions will induce the development of a current sheet along the separatrices, while photospheric motions converging towards the inversion line will favor the formation of a nearly vertical current sheet (see e.g. Fig. 1 in Titov et al. 1993). Due to the reconnection process occurring in the sheet, part of the plasma can be compressed and injected into new and longer field lines, while a large amount can escape downward (see e.g. Low 1996). Then, magnetic reconnection is thought to be able to progressively remove the chromospheric anchorage associated with the presence of very dense plasma in magnetic dips (but a detailed model is still missing). Furthermore, as a fraction of the plasma goes in the upward reconnected field lines, the lighter plasma kept in the dips can be accelerated upward by the magnetic tension. Our observations of the evolution of the Hα arches also agree with this view.

3.4. AFS with two interacting BPs

The magnetic topology associated with the AFS can even be more complex than the one described above with only one BP. The BP shown in the left column of Fig. 4 is indeed formed by two BPs (see Bungey et al. 1996 for the description of the splitting of one BP into two BPs). Figure 6 (top) shows a local zoom of Fig. 4 (left-central panel) centred on the split BP (which we now call BP1 and BP2). The magnetic topology is complex since the separatrices, issued from both BPs, intersect in a line called the separator. A set of field lines rooted in each BP is added to outline the BP separatrices. 3D figures of the same sets of lines from a different point of view are shown in the two central panels. These field lines (see top panel) follow the shape of the observed Hα feature presented in Fig. 3 at 06:52:24 UT (left top).

We propose that the topology of the magnetic field and the physical evolution associated with it (magnetic reconnection at the separator), as described by Bungey et al. (1996), explain well our observations. Photospheric motions force the magnetic configuration to evolve. Because of a complex topology and a high magnetic Reynolds number, this implies first the formation of a current layer; in particular, at the separator location. Magnetic reconnection will occur when this current layer becomes resistively unstable. Field lines close to the separator (see Fig. 6) become closer and reconnect; then, the dense plasma would be compressed in the reconnection region and pushed into the reconnected field lines. The bottom panel of Fig. 6 shows a sketch of one pair of reconnected field lines. The lower reconnected field lines are so small and low-lying (then at least partially covered by the upper ones) that they are unlikely to be observed. Rather what is mainly observed is the set of long reconnected lines.

We may expect to observe some evidence of heating in the SoHO/EIT and *Yohkoh*/SXT loops (Deng et al. 1999) overlaying the region during the reconnection processes described above. Energy release is also expected to occur in secondary reconnections, which are induced after the main reconnection phase and are necessary for the relaxation of the magnetic field (see e.g. Karpen et al. 1998 for a 2.5D numerical simulation

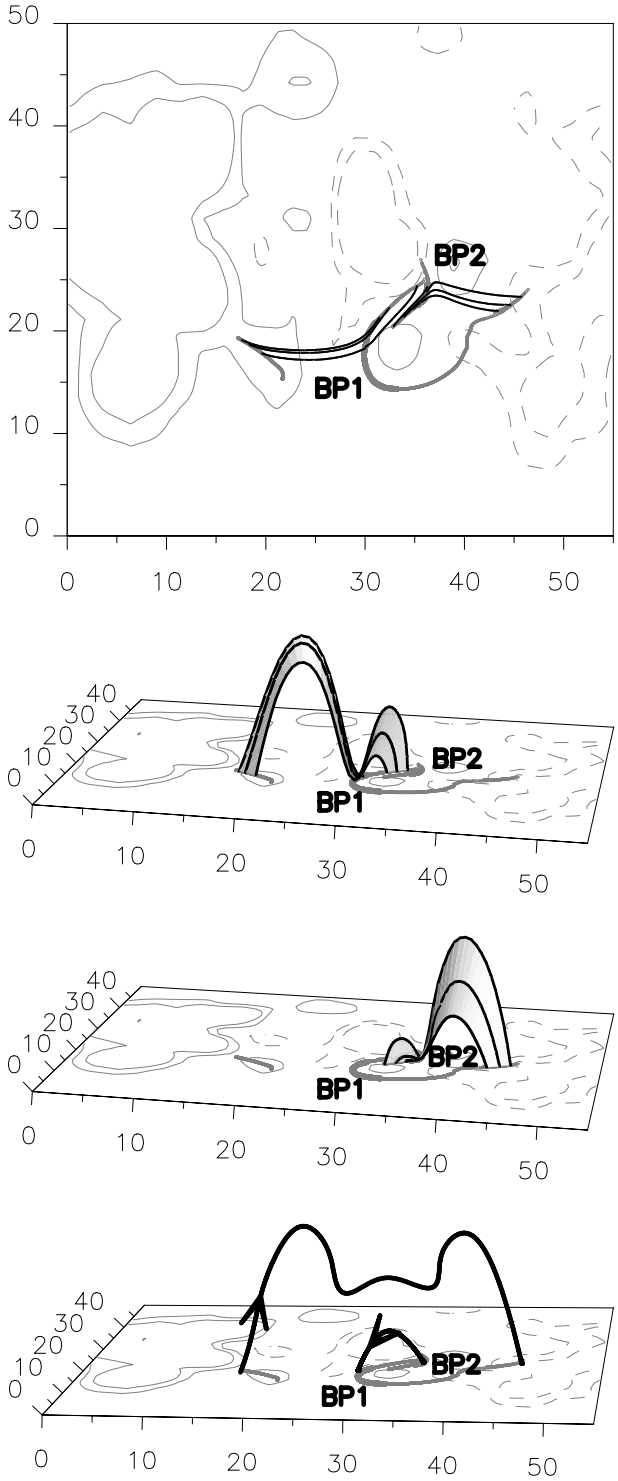

Fig. 6. Model of AR 7968 at 06:28 UT. Top panel shows the location of BPs (thick continuous grey lines) and of the intersection of the associated separatrices with the photosphere (thin continuous grey lines), some field lines (thin black lines) matching the shape of the observed dark arches are added. The two central panels correspond to the set of lines shown above separated in those associated with BP1 and BP2 (for a better presentation the vertical height (z) has been multiplied by a factor 10 and the view point is different from the one used in the top panel). As the field evolves, reconnection between these field lines will occur. The bottom panel shows a sketch of two field lines after reconnection, the longer one represents an elongated fibril, the shorter one would stay below (and is likely to remain unobserved).

of an X-type configuration). Figures 2 and 4 in Deng et al. (1999) show that the core of AR 7968 was brighter in several SoHO/EIT bands, this is likely an effect of higher density at the corresponding temperatures. In Figs. 3 and 5 of the same paper it was shown that very few pixels in the core of the AR have a temperature slightly higher than the average of 2.5×10^6 K, estimated for the full AR; so, no important temperature increase is observed during the early phase of flux emergence in the AR. This can be a consequence of the location of the reconnection region (lower chromosphere where dense plasma is present) and the relatively low energy released (as modeled by Litvinenko & Somov 1994). However, the increase of the plasma density at a given temperature (more precisely in a given wavelength interval) still requires an energy input to heat this plasma from chromospheric temperature to around 10^6 K.

4. The surge on the late phase of AR 7968

4.1. The surge evolution

During June 9, both Hα filtergrams and velocity and intensity maps were obtained at Bialków Observatory. On that day, when the region was already decaying, at about 6:36 UT, a surge was well-observed to the South of the main positive polarity (Fig. 7a). The base of the surge was located towards the East of an emerging region of negative flux. This flux concentration was already present six hours before the event (Fig. 2). The surge extended over a positive flux concentration that had also appeared on that day to the South of the negative one. No flaring activity was observed at that time, only a small zone of enhanced Hα brightness at the base of the surge (as is often the case, Schmieder et al. 1993). During the morning of June 9, the negative polarity extends towards the positive one (see Figs. 2b–d).

From almost the beginning of the event and until about 06:47 UT both red-shifts and blue-shifts could be simultaneously identified at well separated locations. The extension of the blue-shift (white shading in Figs. 7b–d) region gradually decreased with time and the surge became finally mainly red-shifted (black shading in Figs. 7b–d). These red-shifts were seen until 07:27 UT. Figures 7b–d show the evolution of the Hα velocity maps during the surge, together with some intensity contours. The location of the change from red-shifts into blue-shifts lies close to the magnetic inversion line between the two polarities of the new bipole (see Figs. 7b and c and compare to Fig. 2d), taking into account that the inversion line is shifted towards the positive pole (see the location of the BPs in Fig. 8b). It is worth noting that the initial presence of both red-shifts and blue-shifts is not at all the usual scenario. In the standard case (e.g. Schmieder et al. 1996), blue-shifts are observed at the beginning of a surge, followed by red-shifts as the plasma flows back to the chromosphere.

The Dopplershifts calculated in Hα with the chord method (see Sect. 2.1) indicate strong downward velocities of up to 10 km s^{-1}, while the upflows are only of $\approx$1 km s^{-1} in the elongated structures and can reach 3–4 km s^{-1} at the beginning of the event. Strong asymmetries and a broadening of $\approx$25% far away from the line center are present in the Hα profiles. This can be interpreted invoking microturbulence or the existence of emitters with different velocities along the line of sight. The strong bump observed in the wings of the Hα line during the surge can be indicative of higher velocities when using specific techniques of cloud models. Using such a method, the velocities should be multiplied by approximately a factor 4 and could reach up to 40 km s^{-1} (see also Schmieder et al. 1983, 1984). Moreover, these velocities values correspond only to the line of sight component and, due to an important projection effect (see Fig. 9), the plasma velocity amplitude is expected to be higher.

4.2. BPs and the surge on June 9

After modelling the field, we have analyzed in detail its topology in the neighourhood of the surge observed on June 9. Figure 8b shows that two BPs (BP3 and BP4) are present in between the new negative and positive polarities. These BPs define two separatrix surfaces, their intersections with the photosphere is shown in the same figure. Figure 8a depicts a set of field lines associated with BP3 and BP4, the shape of these field lines is in good agreement with the observed surge (compare this figure to Fig. 7a). The topology of the coronal magnetic field is completely described by the two separatrix surfaces, which have a quite complex shape. Moreover, these separatrices intersect (at a separator) as in the magnetic configuration described in Sect. 3.4. In Fig. 8c we have drawn the separator, this particular line belongs to both separatrices and so touches the inversion line twice at the location of BP3 and BP4 (see Bungey et al. 1996).

The origin of surges has been in general associated with magnetic reconnection between a new emerging flux region and the pre-existing magnetic field (see references in Sect. 1). The magnetic configuration is usually simplified to a 2D configuration where magnetic reconnection takes place at an X point.

In this particular case, our topological analysis suggests that the event may be driven by magnetic reconnection occurring at the separator created by the intersection of the separatrices associated with BP3 and BP4. This type of configuration is intrinsically 3 dimensional and cannot be simplified to 2D (the intersection of BP separatrices is not possible in 2D configurations). The evolution of the photospheric field, mainly the changes in the magnetic field intensity and the displacement of the positive polarity to the South of the new negative flux (see Fig. 2), might have started energy release by magnetic reconnection at the separator region (after a current layer was built up there). In a way similar to the case of the chromospheric arches observed at 06:52:24 UT on June 6 (see Sect. 3.4), the dense plasma would be compressed at the reconnection region and injected into the reconnected field lines forming the observed surge. This dense plasma would then flow along the magnetic field lines.

Magnetic field lines associated with BP3 and BP4 are very asymmetric. The ones to the North of both BPs are low (with a maximum height of $\approx$0.6 M derived from the extrapolation) and extremely flat, while those to the South are more steep and

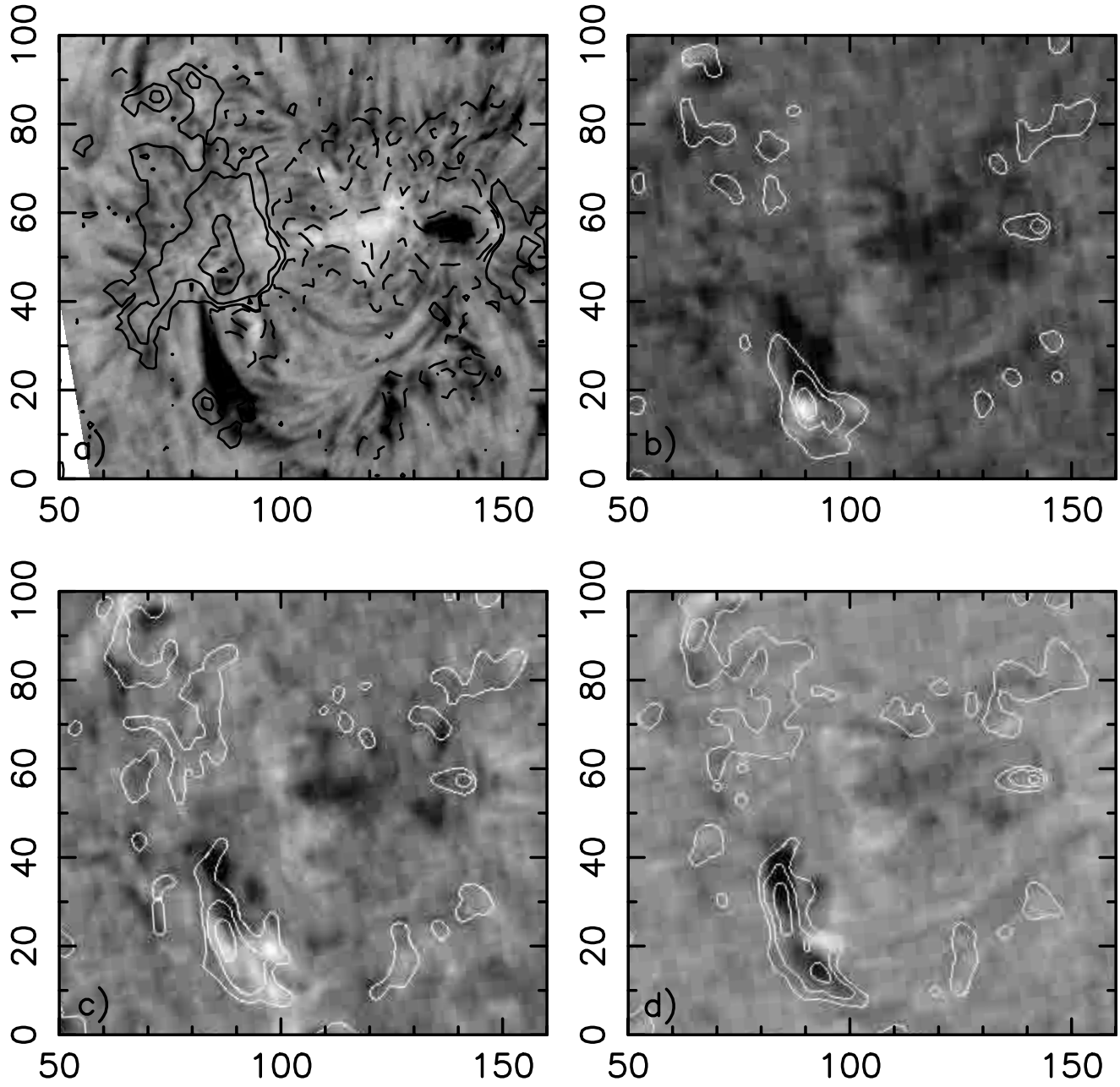

Fig. 7. The surge observed on June 9 in AR 7968. **a)** Filtergram obtained at Bialków Observatory at 06:43 UT. The MDI magnetogram shown in Fig. 2d has been overplotted (the convention for the isocontours is the same as in previous figures). Panels **b)–d)** show the maps of the intensity differences of the blue and red wings of the Hα line during the surge as observed by the MSDP at 06:35:36 UT, 06:40:39 UT and 06:47:03 UT, respectively. Black/white shading corresponds to plasma moving away/towards the observer. Hα line center intensity contours have been superimposed.

higher (with a maximum height of ≈15 Mm). Taking into account this asymmetry and the observer's point of view (see Fig. 9), we expect to see red-shifts towards the northern portion of the surge and blue-shifts towards its southern portion during the early stages of the surge. Finally, we expect to observe red-shifts all along the reconnected loops as the plasma which is not able to overpass the apex of the higher field lines flows back to the chromosphere. This is indeed the evolution observed.

We end this section comparing briefly our results with some of the previously proposed models. In the surge model by Canfield et al. (1996), simultaneous blue-shifts and red-shifts are interpreted as an indication of an initial high twist in the reconnecting magnetic fields (a torsional Alfvén wave is launched after reconnection distributing the initial twist more uniformly in the reconnected field lines). This model presents specific Doppler characteristics: blue-shifts and red-shifts are located at both sides of the longer axis (or extension) of surge (or they are both present at the same locations in unresolved cases). In the case studied by us, the Doppler characteristics are markedly different since the red-shifts and blue-shifts are spatially separated along the surge (top portion and low portion) as

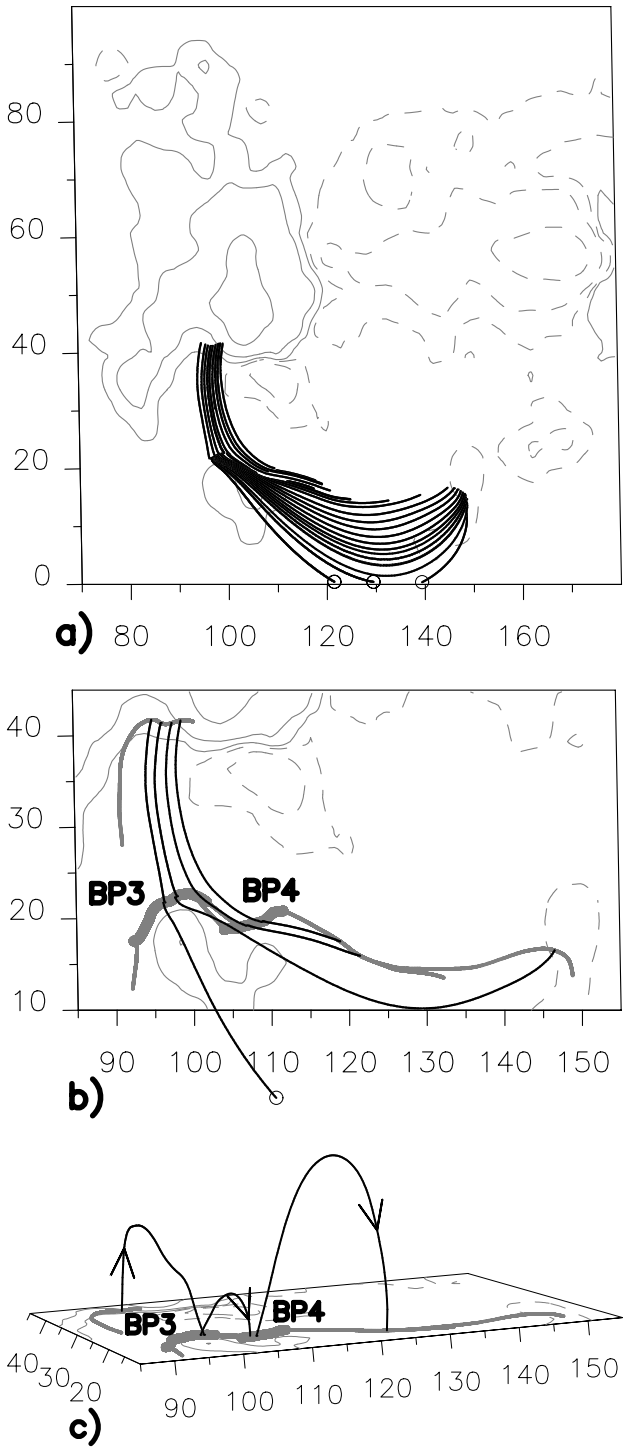

Fig. 8. Magnetic field model of AR 7968. The model corresponds to June 9, 08:40 UT, magnetogram. Panel **a)** shows a set of field lines, issued from the BPs and matching the shape of the observed surge. Panel **b)** depicts the locations of two BPs (called BP3 and BP4) marked with thick grey continuous lines, together with the intersection of their associated separatrices with the photosphere (thin grey continuous lines). Some field lines have been added (black continuous lines). In panel **c)** the magnetic line of intersection between the two separatrix surfaces, the separator, is drawn as a continuous black line (for aesthetics the vertical height (z) has been multiplied by 17 $\sqrt{z}$). Panels **a)** and **b)** correspond to the observer's point of view, while panel **c)** is a different 3D view. The convention for the magnetic field drawing is the same as in Fig. 2.

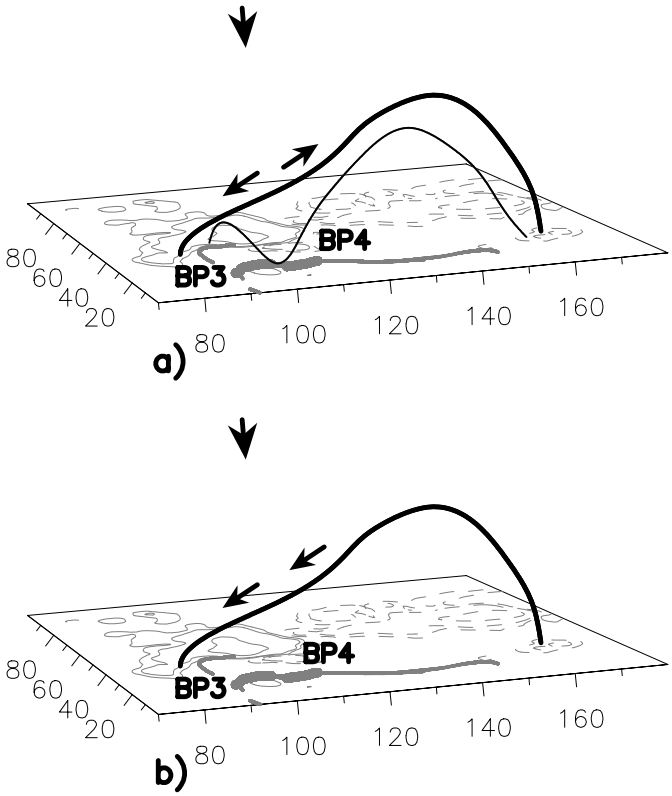

Fig. 9. A sketch of the evolution of the velocities in the surge on June 9. The isocontours represent the June 9, 08:40 UT, magnetogram (BPs and separatrices are added as reference). Panel **a)** corresponds the early stages of the surge. A field line before reconnection is shown with a black continuous thin line. During reconnection, chromospheric plasma will be pushed out of the reconnection region and along the reconnected lines (represented by the continuous black thick line above). Because of the combination between the shape of the reconnected field lines (lower and flatter towards the North, and higher and steeper towards the South, see text) and the point of view (marked in the figure by a large arrow), material will flow away from the observer in the northern portion of the surge and towards the observer in its southern portion (as indicated by the smaller arrows). Panel **b)** shows that, as time proceeds, the plasma that could not overpass the apex of the higher field lines will flow back towards the chromosphere (as shown by the smaller arrows), see Sect. 4.2.

shown in Fig. 7. Furthermore, during June 9, the model of the field matching better the observed loops is close to a potential field without any evidence of twist. Indeed one of the models that, to our knowledge, is the closest to our observations is the MHD simulation of Karpen et al. (1998) where dense material is accelerated at the reconnection site. The main difference with our case is the presence of an X-type (null) point in the initial 2D configuration. In our topological study, we find an intrinsically 3D configuration with a separator not defined by two null points but by the separatrices of two BPs. The magnetic reconnection process associated with this BP separator is expected to have similar characteristics to the simulation described in Karpen et al., but clearly a detailed analysis is required for this BP configuration.

5. Conclusion

This study is focused on the analysis of chromospheric events, evolution of dense AFS and a surge, which are difficult to understand considering the models developed so far. After modelling the magnetic field of the AR, we find that these events are related to the presence of BPs (Bald Patches, which are the portion of magnetic dips tangent to the photosphere). These BPs are stable topological features of the magnetic configuration, since they are present both without or with electric currents and plasma forces (within the limits imposed by the observations to the magnetic field model). Both for an AFS and a surge, we find that the separatrices defined by BPs intersect; so, we have identified in both cases the presence of a separator not associated with magnetic nulls. Such split BP topology was first found theoretically by Bungey et al. (1996). 3D magnetic reconnection is expected to occur at this separator, our observations support this view.

Both AFS and surge associated with the split BP topology have particular characteristics. When the magnetic configuration is not too asymmetric, so that both pre-reconnected loops can be clearly seen, the initial configuration appears as two classical AFSs that later on meet to form one elongated dark Hα structure. The complexity of the magnetic configuration makes the appearance of Hα structures more complex than a single loop (or AFS). Moreover, because the plasma is supported by the magnetic field (upward curvature of field lines), such Hα structure is expected to be denser and of longer duration than the classical AFS. The observations described in this work agree with these expectations but further, more systematic, observations are certainly needed. For the surge case (as for some AFS) associated with the split BP topology, the magnetic configuration is so asymmetric that the shape of the Hα structure alone does not allow us to identify the pre-reconnected loops. However, this type of surge has a marked Dopplershift signature in its initial phase: it spatially changes from red-shift to blue-shift along the surge.

We conclude that magnetic reconnection was at the origin of the evolution observed in both AFS and surge associated to the split BP topology. Magnetic reconnection is presently known to be fast enough at photospheric and chromospheric levels. The faster tearing mode grows with a time scale between 6 and 20 s (Sturrock 1999) and the Sweet-Parker mode is fast enough to explain the observed flux cancellation rate in ARs (Litvinenko & Martin 1999). As in the case of flares, we expect that the spatial location of the main reconnection site is basically determined by the magnetic topology (with a probable dominant role of the separator, when it is present), because the topology determines where current layers will be formed. The upward jet from the reconnection region is likely to be seen as an Hα surge (e.g. MHD simulation of Karpen et al. 1998) if the magnetic tension force is strong enough compared to the gravitational force, i.e. if the reconnection does not occur too deep in the chromosphere. In the opposite case, no jet will be formed, so we will not see a surge; this last case is more relevant to our AFS observations.

Present results can be put in a broader context. Indeed BPs have been found associated with filament feet (e.g. Aulanier et al. 1998b), small flares (Seehafer 1985; Aulanier et al. 1998a) and transition region brightenings (Fletcher et al. 2001). The AFS and surge studied in this paper simply enlarge the list of low energy events that can be associated with the BP topology. This topology is needed to explain the fine structures of these events. However, we are not arguing that a BP configuration is a generic case for AFS and surges, but rather, just another possible configuration (as we have shown previously was possible for UV brightenings and flares). We are indeed only arguing that the magnetic topology, which leads to these phenomena, is broader than what was thought previously and that the BP topology is present in a subset of these events.

Acknowledgements. C.H.M., P.D. and B.S. thank economic support from SETCIP (Argentina) and ECOS (France) through their Argentina – France cooperative science program (A01U04). P.R. has been supported by grant 2.P03D.005.15 of the Polish Committee of Scientific Research. The authors thank the SoHO/MDI consortium for MDI data. SoHO is a joint project by ESA and NASA.

References

Alissandrakis, C. E., Tsiropoula, G., & Mein, P. 1990, A&A, 230, 200
Aly, J. J., & Amari, T. 1997, A&A, 319, 699
Aulanier, G., & Démoulin, P. 1998, A&A, 329, 1125
Aulanier, G., Démoulin, P., Schmieder, B., Fang, C., & Tang, Y. H. 1998a, Sol. Phys., 183, 369
Aulanier, G., Démoulin, P., van Driel-Gesztelyi, L., Mein, P., & DeForest, C. 1998b, A&A, 335, 309
Bungey, T. N., Titov, V. S., & Priest, E. R. 1996, A&A, 308, 223
Canfield, R. C., Reardon, K. P., Leka, K. D., et al. 1996, ApJ, 464, 1016
Chou, D.-Y., & Zirin, H. 1988, ApJ, 333, 420
Delannée, C., & Aulanier, G. 1999, Sol. Phys., 190, 107
Deng, Y. Y., Schmieder, B., Mandrini, C. H., et al. 1999, A&A, 349, 927
Deng, Y. Y., Schmieder, B., Engvold, O., Deluca, E., & Golub, L. 2000, Sol. Phys., 195, 347
Fletcher, L., López Fuentes, M. C., Mandrini, C. H., et al. 2001, Sol. Phys., 203, 255
Georgakilas, A. A., Alissandrakis, C. E., & Zachariadis, T. G. 1990, Sol. Phys., 129, 277
Heyvaerts, J., Priest, E. R., & Rust, D. M. 1977, ApJ, 216, 123
Kurokawa, H., & Kawai, G. 1993, in The Magnetic and Velocity Fields of Solar Active Regions, ed. H. Zirin, G. Ai, & H. Wang, ASP Conf. Ser., 46, 507
Karpen, J. T., Antiochos, S. K., DeVore, C. R., & Golub, L. 1998, ApJ, 495, 491
Litvinenko, Y. E., & Somov, B. V. 1994, Sol. Phys., 151, 265
Litvinenko, Y. E., & Martin, S. F. 1999, Sol. Phys., 190, 45
Low, B. C. 1991, ApJ, 370, 427
Low, B. C. 1992, ApJ, 399, 300
Low, B. C. 1996, Sol. Phys., 167, 217
Low, B. C., & Hundhausen, J. R. 1995, ApJ, 443, 818
Low, B. C., & Wolfson, R. 1988, ApJ, 324, 574
Malherbe, J. M., Schmieder, B., Mein, P., et al. 1998, Sol. Phys., 180, 265
Mandrini, C. H., Deng, Y. Y., Schmieder, B., et al. 1999a, in Proc. 3rd. ASPE, Magnetic Fields and Oscillations, ed. B. Schmieder, A. Hofmann, & J. Staude, ASP Conf. Ser., 184, 276
Mandrini, C. H., Démoulin, P., Schmieder, B., Deng, Y. Y., & Rudawy, P. 1999b, in Proc. 9th, European Meeting on Solar Phys., Magnetic Fields and Solar Processes, ESA SP-448, 617

Mein, P. 1991, A&A, 248, 669
Mein, P., Démoulin, P., Mein, N., et al. 1996, A&A, 305, 343
Rust, D. M. 1968, in Structures and Development of Solar Active Regions, ed. K. O. Kiepenheuer (Dordrecht, D. Reidel), IAU Symp., 35, 77
Rust, D. M., & Kumar, A. 1994, Sol. Phys., 155, 69
Scherrer, P. H., Bogart, R. S., Bush, R. I., et al. 1995, Sol. Phys., 162, 129
Schmieder, B., Vial, J. C., Mein, P., & Tandberg-Hanssen, E. 1983, A&A, 127, 337
Schmieder, B., Mein, P., Martres, M. J., & Tandberg-Hanssen, E. 1984, Sol. Phys., 94, 133
Schmieder, B., Raadu, M. A., & Wiik, J. E. 1991, A&A, 253, 353
Schmieder, B., van Driel-Gesztelyi, L., Gerlei, O., & Simnett, G. 1993, Sol. Phys., 146, 163
Schmieder, B., Malherbe, J. M., Mein, P., et al. 1996, in Magnetic Reconnection in the Solar Atmosphere, ed. C. D. Bentley, & J. T. Mariska, ASP Conf. Ser., 111, 359
Seehafer, N. 1985, Sol. Phys., 96, 307
Seehafer, N. 1986, Sol. Phys., 105, 223
Seehafer, N., & Staude, J. 1980, Sol. Phys., 67, 121
Shibata, K., Nozawa, S., & Matsumoto, R. 1992, PASJ, 44, 265
Spruit, H. C., Title, A. M., & van Ballegooijen, A. A. 1987, Sol. Phys., 110, 115
Steinolfson, R. S., Schmahl, E. J., & Wu, S. T. 1979, Sol. Phys., 63, 187
Sturrock, P. A. 1999, ApJ, 521, 459
Surlantzis, G., Démoulin, P., Heyvaerts, J., & Sauty, C. 1994, A&A, 284, 985
Thomas, J. H. 1988, ApJ, 303, 407
Titov, V. S., Priest, E. R., & Démoulin, P. 1993, A&A, 276, 564
Titov, V. S., & Démoulin, P. 1999, A&A, 351, 707
Tsiropoula, G., Georgakilas, A. A., Alissandrakis, C. E., & Mein, P. 1992, A&A, 262, 587
Vekstein, G. E., Priest, E. R., & Amari, T. 1991, A&A, 243, 492